ELSEVIER

Contents lists available at ScienceDirect

Soil Biology and Biochemistry

journal homepage: www.elsevier.com/locate/soilbio



Microbial community attributes supersede plant and soil parameters in predicting fungal necromass decomposition rates in a 12-tree species common garden experiment

François Maillard ^{a,*}, Briana Beatty ^a, Maria Park ^b, Sylwia Adamczyk ^c, Bartosz Adamczyk ^c, Craig R. See ^{b,d}, Jeannine Cavender-Bares ^b, Sarah E. Hobbie ^b, Peter G. Kennedy ^a

- ^a Department of Plant & Microbiology, University of Minnesota, St. Paul, MN, USA
- ^b Department of Ecology, Evolution and Behavior, University of Minnesota, St. Paul, MN, USA
- ^c Natural Resources Institute Finland, Helsinki, Finland
- d Center for Ecosystem Science and Society, Northern Arizona University, Flagstaff, AZ, USA

ARTICLE INFO

Keywords: Decomposition Microbial residues Forest ecosystems Bacteria Fungi Functional redundancy

ABSTRACT

Although dead fungal mycelium (necromass) represents a key component of biogeochemical cycling in all terrestrial ecosystems, how different ecological factors interact to control necromass decomposition rates remains poorly understood. This study assessed how edaphic parameters, plant traits, and soil microbial community structure predicted the mass loss rates of different fungal necromasses within experimental monocultures of 12 tree species in Minnesota, USA. Necromass decay rates were most strongly driven by initial chemical composition, being significantly slower for fungal necromass with higher initial melanin content. Of the extrinsic ecological factors measured, variation in the amount of mass remaining for both low and high melanin necromass types was significantly predicted by soil bacterial richness and fungal community composition, but not by any soil microclimatic parameters or plant traits. Further, the microbial communities governing decay rates varied depending on the initial necromass chemical composition, suggesting that extrinsic and intrinsic factors interacted to propel decomposition. Finally, we also found significant positive relationships between the amount of remaining fungal necromass and soil carbon and nitrogen concentrations. Collectively, these results suggest that, after the initial chemical composition of dead fungal residues, soil microbial communities represent the main drivers of soil necromass degradation, with potentially large consequences for soil carbon sequestration and nutrient availability.

1. Introduction

Microbial residues (i.e., necromass) represent a key component of forest carbon (C) and nutrient cycles (Buckeridge et al., 2022; Kästner et al., 2021; Sokol et al., 2022), accounting for up to 50% and 80% of soil organic C and nitrogen (N), respectively, across diverse ecosystems (Angst et al., 2021; Liu et al., 2021; Wang et al., 2021). Compositionally, dead fungal mycelium makes up a significantly larger fraction of soil microbial necromass than bacterial residues (Liang et al., 2019; Angst et al., 2021; Wang et al., 2021). The substantial contribution of fungal necromass to soil C and N stocks can be principally explained by the fast turnover of fungal mycelium relative to plant tissues (See et al., 2022), as well as the capacity of molecules deriving from necromass to form

stable bonds with mineral particles (Cotrufo et al., 2013; Liang et al., 2017) and organic compounds (Buckeridge et al., 2020). Furthermore, fungal necromass can also accrue in particulate forms in the soil (Fernandez et al., 2019; Maillard et al., 2021), as fungal necromass quickly reaches a plateau phase in terms of mass loss (Ryan et al., 2020; Schweigert et al., 2015; See et al., 2021).

The asymptotic nature of fungal residue decomposition corresponds closely with changes in fungal necromass chemical composition; fungal residues rapidly lose labile compounds during the first phases of decomposition (up to three months) and then retain a significant fraction in later stages that appear to be resistant to microbial degradation (Fernandez et al., 2019). Therefore, after a phase of rapid mass loss post-senescence, fungal necromass mass remaining stabilizes, and the

E-mail address: francois.maillard2@gmail.com (F. Maillard).

^{*} Corresponding author.

decay rates almost reach zero (Ryan et al., 2020; Maillard et al., 2021; See et al., 2021). Of the intrinsic factors (i.e., properties of the fungal necromass itself) influencing fungal residue decomposition, melanin, an abundant pigment detected in the cell walls of two-thirds of soil fungi (Siletti et al., 2017; van der Wal et al., 2009), has been consistently associated with the persistence of fungal residues in the late stages of decomposition (Fernandez and Koide, 2014; Fernandez and Kennedy 2018; Maillard et al., 2023). Indeed, the level of melanization of fungal necromass is highly predictive of the amount of necromass remaining (Beidler et al., 2020; Fernandez et al., 2019) as well as of soil C stocks (Clemmensen et al., 2015; Siletti et al., 2017).

Compared to intrinsic factors such as melanin, the influence of extrinsic factors (i.e., characteristics of the biotic or abiotic environment) on fungal residue decomposition remains largely unexplored (see Beidler et al., 2020 for rare exception). Given that these factors have been extensively described as controlling the decomposition rates of plant-derived organic matter, it seems likely they may also affect fungal residue degradation (Bradford et al., 2016; Fanin et al., 2020; Maillard et al., 2022a; Prescott 2010; Vivanco and Austin 2008). Additionally, understanding how extrinsic factors affecting fungal residue accumulation interact with dead mycelial chemical properties is crucial for improving the incorporation of microbial necromass decomposition into forest soil biogeochemical models (Wieder et al., 2015).

Of the extrinsic factors influencing necromass decomposition rates, abiotic and biotic properties are likely both important. Concerning the former, Fernandez et al. (2019) found that fungal necromass incubated in experimentally warmed plots decomposed faster than under ambient conditions, consistent with other observations showing greater microbial necromass decomposition in warmer study systems (Throckmorton et al., 2012). Combining laboratory and field experiments, Adamczyk et al. (2019) revealed that tannins deriving from tree roots acted as an extrinsic biotic factor decelerating fungal residue degradation. By complexing with necromass-associated proteins, likely with chitin polymers, and with enzymes involved in decomposition, plant tannins were found to inhibit microbial degradation of fungal necromass, contributing to its stabilization in the soil (Adamczyk et al., 2017, 2019; Hättenschwiler et al., 2019). Similarly, root-associated fungi, notably ectomycorrhizal fungi, have been associated with a deceleration in fungal necromass decomposition (Beidler et al., 2021; Maillard et al., 2021). While the mechanisms underpinning this deceleration remain unknown, they might be related to competition between saprotrophic microbes and ectomycorrhizal fungi for organic nutrients deriving from mycelial residues (Fernandez and Kennedy, 2016).

With regard to the microbial communities present on decaying fungal necromass, Maillard et al. (2021) recently demonstrated that the abundance of several bacterial and fungal genera colonizing dead fungal mycelia was significantly associated with the necromass decay rate. Most notably, the early stages of decomposition are typically dominated by copiotrophic bacteria, which likely thrive on the labile compounds of necromass. Conversely, the late stages of decay oligotrophic bacteria become the most abundant, which are more efficient at degrading resistant compounds (Beidler et al., 2020; Maillard et al., 2021). Nevertheless, because microbial communities change rapidly during fungal necromass decomposition (Beidler et al., 2020; Brabcová et al., 2016, 2018; Kennedy and Maillard 2022; Maillard et al., 2022b), the relationships between mass loss and microbial taxa abundance might simply be associated with a successional pattern that doesn't relate to specific bacterial or fungal degradation activities, but rather to other factors influencing the microbial community structure, such as microbial interactions (e.g., antibiotics production, mycoparasitism, spatial competition). Researchers have also incubated fungal necromass in various habitats and forest types (soil vs. leaf litter for Brabcová et al., 2016; soil vs. dead wood for Maillard et al., 2020; ectomycorrhizal or arbuscular mycorrhizal forests for Beidler et al., 2021) to assess how potential differences in microbial community composition may influence fungal residue decomposition. Those studies found the amount of necromass remaining in the late stages of decomposition to be surprisingly similar between habitats (Brabcová et al., 2016; Maillard et al., 2020) and forest types (Beidler et al., 2021), suggesting a high functional redundancy of the microbial communities involved in necromass decomposition. Nonetheless, different incubation niches and forest types typically have large differences in edaphic and microclimatic parameters that may also potentially influence necromass decomposition rates, thus limiting conclusions about the specific role of soil microbes in fungal necromass degradation.

In this study, we took advantage of a common garden experiment containing 12 tree species representative of the North America temperate forests, which had been grown in monoculture for 9 years at the same experimental site in Minnesota, USA (Grossman et al., 2020). We first assessed a range of abiotic and biotic extrinsic factors possibly driving fungal necromass decomposition rates based on the existing literature, which included soil parameters (pH, temperature, and moisture), tree traits (fine root density, and fine root and leaf tannin contents), and soil bacterial and fungal community richness and composition. We chose soil microbial communities as potential predictors of fungal necromass decomposition rates since they have been described as relatively stable in forest ecosystems regarding richness and composition across seasons (Martinović et al., 2021; Santalahti et al., 2016; Shigyo et al., 2019). We then incubated fungal residues with low or high melanin content in the same tree plots in which edaphic, plant, and microbial parameters were quantified. After five months of incubation in soil, the amount of necromass remaining was determined, corresponding to the late stages of decomposition in terms of mass loss (Ryan et al., 2020; See et al., 2021). Then, we used a multimodel inference approach to determine the best predictors for the low and high melanin necromass decomposition rates. Finally, we tested the relationships between soil C and N concentrations and fungal necromass decay rates (i.e., the amount of fungal necromass remaining after five months of decomposition).

We hypothesized the following:

- **H1.** Plots with elevated temperature and moisture levels (due to variations in tree traits such as canopy height, canopy light interception, water use, and litter layer depth) would favor the activity of microbial decomposers and accelerate decomposition for both necromass types.
- **H2.** Tree species with high tannin concentrations in their fine roots and leaves would be associated with low decomposition rates for both necromass types.
- **H3.** Tree species hosting ectomycorrhizal fungi would be associated with lower rates of necromass decomposition, while plots harboring a high richness and abundance of soil copiotrophic bacteria and saprotrophic fungi would be related to fast necromass decomposition rates.
- **H4.** Tree species hosting ectomycorrhizal fungi would be associated with higher soil C concentration, and low necromass decomposition rates would be linked with higher soil C concentration.

2. Materials and methods

2.1. Field site

We conducted our study at the Forests and Biodiversity experiment (FAB; Grossman et al., 2017) at the Cedar Creek Ecosystem Science Reserve (Cedar Creek), a 2300-ha reserve and National Science Foundation Long-Term Ecological Research site in eastern Minnesota, in the United States (45°25′ N, 93°10′ W). The site is situated on the Anoka Sand Plain, which is characterized by excessively drained soils consisting of upwards of 90% sand. The mean annual temperature at Cedar Creek is 6.7 °C, and the mean annual precipitation is 801 mm. The experimental site consists of a common garden experiment in which 12 tree species were planted in 2013 in mono- and polyculture combinations. Four of these species are gymnosperms: eastern red cedar

(Juniperus virginiana), and white (Pinus strobus), red (P. resinosa), and jack (P. banksiana) pine. The eight angiosperm species include red (Quercus rubra), pin (Q. ellipsoidalis), white (Q. alba), and bur (Q. macrocarpa) oak; red maple (Acer rubrum) and box elder (A. negundo); paper birch (Betula papyrifera); and basswood (Tilia americana). Among the 12 studied tree species, three established symbiotic interactions with arbuscular mycorrhizal fungi (J. virginiana, A. rubrum, and A. negundo), and nine with ectomycorrhizal fungi (B. papyrifera, Q. alba, Q. ellipsoidalis, Q. macrocarpa, Q. rubra, P. banksiana, P. resinosa, P. strobus, and T. americana). Each of the three blocks of the experiment (spaced 4.5-m apart) consisted of either 46 or 47 square plots with a side of 3.5 m; plots were planted with 1, 2, 5, or 12 species. Each plot contained 64 trees, planted at 0.5-m intervals. Here, we focused on the monospecific plots (n = 36 with three plots per tree species) (see Grossman et al., 2017 for details about the experimental site). We excluded two plots of A. negundo and one plot of A. rubrum that had exceptionally high mortality rates. Consequently, the remaining A. negundo plot was subdivided into three subplots while one of the two remaining A. rubrum plots was randomly chosen and divided into two subplots.

2.2. Soil sampling

On June 29, 2021, we sampled soil cores (6-cm diameter) at each monocultural plot (n = 36). Prior to coring, the organic horizon containing decomposed materials was carefully removed to collect the forest topsoil (0–5 cm) exclusively. Two cores were randomly taken from each plot and pooled in the field, while avoiding plot borders to limit edge effects. The soil samples were placed in a cooler and then held at 4 $^{\circ}\mathrm{C}$ in the laboratory until processing (within one day). The soil samples were sieved (2 mm), and the tree roots were collected for fine-root density quantification. An aliquot of each soil sample was freeze-dried for molecular analyses.

2.3. Edaphic parameters

A sub-sample of the soil from each plot was air-dried and analyzed in double distilled water with a benchtop pH meter to determine the pH. The topsoil temperature and moisture content were measured in the field on August 9, 2021, using a soil time-domain reflectometry (TDR) sensor (FieldScout TDR, Spectrum Technologies Inc., USA) and a soil thermometer. Soil temperature and water measurements were determined at four random places for each monospecific tree plot, and the results were averaged. We also determined mineral soil C and N concentrations to 20 cm depth using five 20 cm 2 cores collected from each plot in July 2019. Cores were composited by plot, wet sieved (2 mm), and dried at 105 °C prior to analysis. Soil C and N concentrations were determined by dry combustion (Costech Analytical Technologies Inc.).

2.4. Tree traits

Tree roots sorted from the soil samples were washed thoroughly with water. Fine roots (below 2 mm in diameter, Liu et al., 2018) were excised and freeze-dried. No sign of root zone overlap from tree species of surrounding plots were noticed during this step. Further, we calculated the fine-root density for each plot as the g of dry biomass of fine root per m³ of topsoil. Freeze-dried fine roots were subsequently used for root tannin quantification. Tannin concentrations (sum of condensed tannins and hydrolysable tannins) were measured using the protein precipitating method as described in Adamczyk et al. (2008). Briefly, after extraction with acetone-water (7:3), followed by reaction with protein, tannin concentrations are determined spectrophotometrically based on oxidation of hydroxyl groups with FeCl³ and formation of iron-phenolate complex. Tannic acid (Sigma Chemicals), characterized as in Adamczyk et al. (2017), was used as the standard. Samples were measured in two technical replicates. The final results are presented as

milligrams of tannic acid equivalents per gram of dry fine root material. For leaf tannin concentrations, we used data collected by Grossman et al. (2020) in a previous experiment conducted at the same experimental site.

2.5. Soil microbial analyses

We used high throughput sequencing (HTS) of bacterial (16S) and fungal (ITS) taxonomic markers to characterize microbial community richness and structure. In total, 36 soil samples were analyzed (three per tree monospecific plots). Total genomic DNA was extracted with PowerSoil Pro kits (MoBio, Carlsbad, CA, USA) from 0.25 g of freeze-dried soil following the manufacturer's instructions. DNA extraction (lysis tubes with no substrate added) and PCR blanks (molecular-grade water as a replacement for template DNA) were also included. For bacteria, the 515F-806R primer pair was chosen to target the V4 region of the 16S rRNA gene (Caporaso et al., 2012). For fungi, the 5.8S-Fun and ITS4-Fun primer pair (Taylor et al., 2016) was used to target the ITS2 region of the fungal rRNA operon. Samples were first amplified in individual 20 μ l reactions containing 10 µl of Phusion Hot Start II High-Fidelity PCR Master Mix (Thermo Scientific, Waltham, MA, USA), 0.5 µl of each 20 mM primer, 1 µl of DNA template and 8 µl of PCR-grade water. Thermocycling conditions were as follows: 1) 98 °C for 30 s, 2) 98 °C for 30 s, 3) 55 $^{\circ}$ C for 30 s, 4) 72 $^{\circ}$ C for 30 s, repeat steps 2–4 34 times, 5) 72 $^{\circ}$ C for 10 min and 6) infinite hold at 4 °C. If initial PCRs were not successful, template DNA dilutions were performed. For all samples with amplicons, a second PCR was run under thermocycling conditions to add unique Golay barcodes and sequencing adaptors. PCR products were then cleaned using the Charm Just-a-Plate Purification and Normalization Kit (Charm Biotech, San Diego, CA, USA). Each sample was then pooled at equimolar concentration and sequenced with the MiSeq technology (2 × 250 bp V2 Illumina chemistry) at the University of Minnesota Genomics Center. Raw.fastq files for each sample were deposited in the NCBI Short Read Archive as bioproject PRJNA916697.

Sequences were bioinformatically processed using the AMPtk pipeline v1.4.2 (Palmer et al., 2018). A quality assessment of a fungal mock community sample revealed that including reverse reads in the following pipeline notably lowered OTU richness as well as the total sequence reads per OTU (likely due to poor quality). To avoid this data loss, we used only the forward reads for both the bacterial and fungal datasets. Sequences first had primers removed and were all trimmed 250 bp. They were next denoised with the DADA2 algorithm (Callahan et al., 2016) and the resulting ASVs were clustered into operational taxonomic units (OTUs) at 97% similarity. A 0.5% abundance cut-off was applied to eliminate very low abundance OTUs that likely resulted from barcode index-bleed (Palmer et al., 2018). Taxonomy was assigned using a hybrid algorithm integrating results from a USEARCH global alignment against the RDP (bacteria) and UNITE (fungi) databases, respectively, with both UTAX and SINTAX classifiers.

From the bacterial dataset, we removed any OTUs lacking a kingdom identity (i.e., not being classified as bacterial sequences) and being classified as mitochondrial or chloroplastic organelles. We excluded any OTUs with no fungal taxonomic annotations from the fungal dataset. We then summed OTU sequence reads detected as contaminants in either the extraction and PCR blanks for the bacterial and fungal datasets and subtracted those sums from the environmental samples. Finally, to account for variation in total sequence read counts across samples, all analyses were based on counts rarefied to 1,966 per sample and 16,692 per sample for the bacterial and the fungal datasets, respectively (see Fig. S1 for the bacterial and fungal OTU accumulation curves). Good's coverage index was calculated for each sample. All the samples presented scores above 0.97 and 0.99 for the bacterial and fungal datasets, respectively, which was deemed suitable for subsequent analyses. Following quality filtering and rarefaction, all samples were retained (n = 36 for both the bacterial and fungal communities), which represented a total of 70,776 and 600,912 sequences belonging to 1,565 bacterial

and 1,117 fungal OTUs, respectively.

Bacterial OTUs were assigned to copiotrophic and oligotrophic functional groups based on Li et al. (2021). Specifically, all bacterial OTUs belonging to the phylum Bacteroidetes, Firmicutes, Gemmatimonadetes, and classes alpha-Proteobacteria, and gamma-Proteobacteria were defined as copiotrophic, while bacterial OTUs belonging to phylum Acidobacteria, Actinobacteria, Planctomycetes, Chloroflexi and class delta-Proteobacteria were defined as oligotrophic. Trophic mode assignments for fungi were made with FUNGuild (Nguyen et al., 2016). For the fungi, we restricted our analyses to ectomycorrhizal and saprotrophic fungi, which dominated our dataset in comparison to other fungal guilds (Table 1).

2.6. Mycobag preparation, deployment, and collection

To determine the decomposition rates of fungal residues, we used the species Meliniomyces bicolor as our source of necromass because it is a naturally present soil species in temperate and boreal forests (Grelet et al., 2009) and can have its melanin content manipulated in the laboratory non-chemically (Fernandez and Kennedy, 2018). Following the protocol described by Fernandez and Kennedy (2018), we produced two types of M. bicolor mycelial residues in axenic conditions, hereafter referred to as low and high melanin necromass (see Table S1 for the chemical profiles of the two *M. bicolor* necromass types used in this study based on Fernandez and Kennedy, 2018). For both necromass types, we homogenized and freeze-dried the fungal necromass separately (100 mg dry matter; low and high melanin necromass) and then placed them in polyester mesh bags (5 \times 10 cm, with 53- μ m pores) (R510 Forage Bag, ANKOM Technology, Macedon, NY, USA), followed by and heat-sealing. The 53-µm mesh size excluded tree root in-growth and did not allow for the penetration of soil particles, making it suitable for the quantification of fungal necromass degradation rates (Beidler et al., 2020). On the same day as soil sampling for predictor variable quantification (June 9, 2021), immediately after soil coring, we deployed the mycobags. Within each monocultural tree plot, two sets of low and high melanin mycobags (n = 72 for each necromass type) were buried in the topsoil (0–5 cm depth) at a randomly chosen position while avoiding plot borders to limit edge effects.

After five months of incubation, on November 2, 2021, corresponding to the late stage of fungal necromass decomposition when mass loss decay rates approached zero (See et al., 2021), we harvested the mycobags. The mycobags were individually bagged, placed on ice, and taken to the laboratory for immediate processing. Among the 144 bags deployed, three bags were not included in the analysis (two were lost, and one was found unburied at harvesting). In the laboratory, fungal necromass was carefully removed using sterile pipette tips for each sample, transferred in autoclaved tubes (2 ml), and stored at −80 °C until freeze drying. We pooled the necromass of the same quality (low or high melanin necromass) from the two sets incubated at each plot to account for spatial variations in necromass decomposition at the plot level. Necromass decomposition rates for each plot and necromass type (low and high melanin) were expressed as the percent of initial mass remaining. Based on the results presented in Beidler et al. (2020), any loss-on-handling during necromass deployment was considered negligible.

2.7. Data analyses

Statistical analyses and data visualization were performed using R software (R Core Team, 2020). All tests were considered significant using a threshold of P < 0.05. An analysis of variance (ANOVA) was used to test for differences in fungal necromass mass remaining depending on necromass quality (low and high melanin) and tree species (A. negundo, A. rubrum, B. papyrifera, J. virginiana, P. banksiana, P. resinosa, P. strobus, Q. alba, Q. ellipsoidalis, Q. macrocarpa, Q. rubra, and T. Americana). Before the ANOVAs, the residual variances were tested for

homoscedasticity using Cochran's test, and data were log-transformed if necessary. In parallel, we used linear mixed-effect models with the lme4 package (Bates et al., 2015) to analyze the differences in fungal necromass mass remaining depending on necromass type (low or high melanin), tree phylogeny (angiosperm or gymnosperm species), and tree mycorrhizal association (arbuscular mycorrhizal and ectomycorrhizal fungal), with the tree species designated as a random factor. The ANOVA was then applied to the linear mixed-effect models to test for fixed effects (necromass type, tree phylogeny, and tree mycorrhizal association).

The effects of tree species on the soil bacterial and fungal communities were tested using permutational multivariate analyses of variance (PERMANOVA) and visualized with a principal coordinate analysis (PCoA). We calculated the overall bacterial and fungal operational taxonomic unit (OTU) richness as well as the functional group OTU richness (bacteria; oligotroph, copiotroph, or unclassified, fungi; ectomycorrhizal, saprotroph, or unclassified) using the Vegan package for R (Oksanen et al., 2013). The relative abundance of the bacterial and fungal functional groups was also quantified. We used one-way ANOVAs followed by Tukey's honest significance test to evaluate the effects of tree species on the edaphic (soil pH, moisture, and temperature), plant (fine-root density, and fine-root and leaf tannin concentrations), bacterial (OTU richness, functional group OTU richness and abundance) parameters.

To determine the best predictors of fungal necromass decomposition rates, we used information theory model selection in the MuMIn package for the low and high melanin necromass types separately (i.e., response variables) (Burnham and Anderson, 2002). We included 19 predictor variables belonging to edaphic (pH, moisture, and temperature), plant (fine root density, and fine root and leaf tannin concentrations), soil microbial richness (bacterial and fungal total, and separated by functional group OTU richness), soil microbial functional group abundance (bacterial and fungal functional group relative abundances), and soil microbial community structure (bacterial and fungal PCoA axis 1 and 2). The response and predictor variables were rescaled, and we used the lm function to fit a basic linear model for each response variable (i.e., low or high melanin necromass mass remaining). We then generated a full set of models for the low and high melanin necromass decomposition rates, from which we selected all those within four AICc units of the best-fitting model (i.e., with the lowest AICc score). Model-averaged coefficients and the relative importance values for the predictors were calculated from the selected models for each response variable (i.e., low or high melanin necromass mass remaining). All significant predictor variables were tested for relationships with fungal necromass decomposition rates using Pearson's correlations. We also used canonical correspondence analysis (CCA) from the Vegan R package to identify correlations between the most abundant fungal genera (top 50 genera) and fungal necromass decomposition rates, with the low and high melanin necromass mass remaining used as predictors. Finally, we tested the relationships between soil C and N concentrations and the necromass decay rates using Pearson's correlations.

3. Results

3.1. Effect of tree species on the edaphic, plant, and soil microbial parameters

Tree species had no significant effect on soil pH (P=0.36), but significantly affected both soil moisture (P<0.001) and temperature (P=0.011, Table 1). Soil moisture ranged from 5.66 to 15.43% across tree species, being, on average, lowest for the *Pinus* species, intermediate for *B. papyrifera* and *J. virginiana*, and the highest for *T. americana*, and *Acer* and *Quercus*. The range of soil temperatures under different tree species was narrower (18.88–20.75 °C on average), with soil temperatures being consistently cooler for all the *Pinus* species.

	Predictor	Tree species effect	Acer negundo	Acer rubrum	Betula papyrifera	Juniperus virginiana	Pinus banksiana	Pinus resinosa	Pinus strobus	Quercus alba	Quercus ellipsoidalis	Quercus macrocarpa	Quercus rubra	Tilia americana
Soil	pH	F1.157, P =	$6.33 \pm$	6.08 \pm	$6\pm0.07~\text{a}$	6.05 ± 0.09	$6.12~\pm$	5.97 \pm	6.21 \pm	$6.29 \pm$	5.93 ± 0.19	6.08 ± 0.14	$6.15~\pm$	6.05 ± 0.12
		0.365	0.11 a	0.07 a		a	0.06 a	0.09 a	0.15 a	0.11 a	a	a	0.08 a	a
	Moisture (%)	F6.937, P <	$11.25~\pm$	15.43 \pm	9.4 ± 0.39	9.53 ± 1.16	$5.66 \pm$	7.03 \pm	7.61 \pm	$11.53~\pm$	$11.22~\pm$	11.13 ± 0.85	11.71 \pm	12.51 ± 1.2
		0.001***	0 abc	1.27 a	bcd	bcd	0.78 d	0.52 cd	1.22 bcd	1.34 abc	0.47 abc	abc	1.63 abc	ab
	Temperature (°C)	F3.021, P =	$20.75~\pm$	19.43 \pm	19.34 \pm	19.07 \pm	18.88 \pm	18.98 \pm	18.42 \pm	19.48 \pm	19.76 \pm	19.07 ± 0.33	19.48 \pm	19.28 \pm
		0.011*	0 a	0.73 ab	0.28 ab	0.13 b	0.29 b	0.07 b	0.37 b	0.14 ab	0.08 ab	b	0.49 ab	0.22 ab
Plant	Fine root density (g/m3)	F22.57, P <	7.14 ±	3.44 \pm	$18.85 \pm$	47.28 \pm	42.34 \pm	29.41 \pm	$18.90 \pm$	$9.15 \pm$	9.47 ± 1.04	10.07 ± 2.07	$14.30 \pm$	18.55 \pm
		0.001***	1.86 de	0.55 e	1.81 cd	4.15 a	3.30 ab	1.39 bc	2.70 cd	4.28 de	de	de	4.56 de	3.74 cd
	Fine root tannin (mg/g)	F15.57, P <	88.73 \pm	63.62 \pm	92.18 \pm	68.24 \pm	53.84 \pm	48.1 \pm	37.44 \pm	54.96 \pm	$\textbf{85.98} \pm \textbf{5.8}$	99.24 ± 4.88	58.34 \pm	37.52 \pm
		0.001***	8.39 abc	4.72 cde	6.73 ab	3.38 bcd	7.53 de	4.54 de	4.05 e	3.69 de	abc	a	4.13 de	4.28 e
	Leaf tannin (mg/g)	not	69.9	46.9	54.2	19.7	183.2	221.0	77.1	38.6	68.3	50.1	39.6	121.3
Bacteria	OTU richness (number of	applicable $F0.8, P = 0.64$	374 ±	$316 \pm$	407.67 ±	374 \pm	388.67 \pm	399.33 \pm	$397 \pm$	405 ±	$361.67 \pm$	371 ± 12.22	$377.33~\pm$	323.33 \pm
	OTUs)	10.0,1 0.01	17.16 a	72.06 a	5.9 a	21.08 a	26.27 a	11.86 a	38.4 a	34.02 a	40.58 a	a	15.3 a	40.13 a
	Oligotrophic OTU	F0.818, P =	183.67 ±	152 ±	193.67 ±	188.33 ±	180.67 ±	197.67 \pm	192.33 \pm	187 ±	176.67 ±	$165.67 \pm$	180.33 ±	157.33 ±
	richness (number of	0.624	7.88 a	37.03 a	8.51 a	6.17 a	7.86 a	11.85 a	19.1 a	12.58 a	17.57 a	3.38 a	8.09 a	20.2 a
	OTUs)													
	Copiotrophic OTU	F2.05, P =	89 ± 7.57	74.67 \pm	121 ± 3.51	91.33 \pm	116.67 \pm	104.67 \pm	$115~\pm$	114.33 \pm	93.67 \pm	102.67 \pm	94.33 \pm	76 ± 12.17
	richness (number of OTUs)	0.0686	a	19.33 a	a	13.04 a	11.32 a	1.2 a	12.12 a	13.92 a	9.67 a	6.12 a	7.26 a	a
	Oligotrophic abundance	F4.986, P <	$34.13~\pm$	$31.79 \pm$	37.08 \pm	34.71 \pm	44.47 \pm	38.59 \pm	48.78 \pm	37.47 \pm	$36.15~\pm$	32.49 ± 0.14	33.67 \pm	32.76 \pm
	(%)	0.001***	0.21 bc	4.52 c	3.27 bc	2.05 bc	2.45 ab	1.65 abc	1.69 a	1.37 abc	1.01 bc	c	2.05 bc	2.98 c
	Copiotrophic abundance	F2.934, P =	12.44 \pm	10.85 \pm	20.06 \pm	11.21 \pm	26.36 \pm	17.68 \pm	22.57 \pm	19.31 \pm	17.82 \pm	12.77 ± 0.76	12.02 \pm	9.27 ± 1.41
	(%)	0.0133*	1.66 ab	3.27 ab	1.01 ab	1.56 ab	5.11 a	2.36 ab	1.01 ab	5.31 ab	6.11 ab	ab	0.66 ab	b
Fungi	OTU richness (number of	F3.13, P =	252.67 \pm	331.67 \pm	$167~\pm$	283.33 \pm	221.67 \pm	249.33 \pm	200 \pm	231 \pm	257.67 \pm	223.33 \pm	290 \pm	219.67 \pm
	OTUs)	0.00939**	44.37 ab	10.65 a	10.39 b	14.44 ab	16.7 ab	5.61 ab	22.61 b	17.62 ab	40.92 ab	26.41 ab	27.74 ab	26.74 ab
	Ectomycorrhizal OTU	F2.839, P =	$3\pm1\;b$	4 \pm 1 ab	12.33 \pm	4.67 ± 4.18	7.67 \pm	$10\pm1~\text{ab}$	10.67 \pm	$\textbf{9.67} \pm \textbf{2.4}$	$16\pm3~\text{a}$	10.33 ± 1.45	16 ± 3.21	10 ± 3.46
	richness (number of OTUs)	0.0158*			3.18 ab	ab	1.33 ab		1.76 ab	ab		ab	a	ab
	Saprotrophic OTU	F2.601, P =	$105 \pm$	140 \pm	77 ± 0 b	110 ± 8.5	98 ± 8.72	106.67 \pm	95 ±	100.67 \pm	$112.67~\pm$	$98\pm10~ab$	125.33 \pm	88 ± 14.11
	richness (number of OTUs)	0.0244*	16.62 ab	7.55 a		ab	ab	5.24 ab	11.15 ab	6.36 ab	13.12 ab		10.91 ab	ab
	Ectomycorrhizal	F1.426, P =	13.7 \pm	7.55 \pm	51.14 \pm	$21.73~\pm$	5.99 ±	49.77 \pm	45.9 ±	$35.28 \pm$	46 ± 19.91 a	59.14 \pm	46.78 \pm	35.28 \pm
	abundance (%)	0.225	8.39 a	5.63 a	16.17 a	21.73 a	1.31 a	12.35 a	14.49 a	17.92 a		12.52 a	11.33 a	24.54 a
	Saprotrophic abundance	F1.807, P =	$51.79 \pm$	60.27 \pm	40.74 \pm	45.44 ± 11	77.73 \pm	36.78 \pm	44.61 \pm	33.98 \pm	31.38 \pm	$29.99 \; \pm$	35.09 ± 7	39.83 \pm
	(%)	0.109	7.34 a	3.84 a	12.69 a	a	2.45 a	8.39 a	13.76 a	9.38 a	11.57 a	10.39 a	a	16.17 a

Tree fine root density and tannin content significantly differed among tree species (P < 0.001 for both) (Table 1). Across species, the fine root densities were relatively low, around or below 10 g m⁻³ for A. negundo, A rubrum, Q. alba, Q. ellipsoidalis, and Q. macrocarpa; high, above 40 g m⁻³ for J. virginiana, P. banksiana, and P. resinosa; and intermediate for B. papyrifera, P. strobus, P. resinosa, Q. rubra, and P. resinosa, P. r

Soil bacterial and fungal community structure was significantly impacted by tree species (P < 0.001), explaining 44% and 45% of bacterial and fungal OTU composition, respectively (Fig. S2). Based on PCoA visualization, there was no consistent clustering by tree genera, mycorrhizal association (arbuscular mycorrhizal vs. ectomycorrhizal), or phylogeny (angiosperm vs. gymnosperm) for the bacterial communities. The PCoA fungal communities showed some clustering by tree genus, with the different Acer, Quercus, and Pinus species-associated communities being relatively closer together. However, we again did not find any grouping of the fungal community composition by mycorrhizal association or phylogeny. Permutational multivariate analyses (PERMANOVA) revealed that soil moisture (P < 0.010) and leaf tannin (P < 0.016) significantly affected the structure of the soil bacterial communities (Table S3). Soil fungal OTU composition was significantly impacted by soil moisture (P < 0.005), temperature (P < 0.034), fine root density (P < 0.043), and leaf tannin (P < 0.002).

Tree species had no effect on the total bacterial (P=0.64), oligotrophic (P=0.62) or copiotrophic (P=0.07) OTU richness (Table 1). The relative abundance of oligotrophic bacteria was significantly different among tree species (P<0.001) and notably high for the three *Pinus* species. The total fungal (P<0.01), ectomycorrhizal ECM (P<0.05) and saprotrophic (P<0.05) OTU richness changed significantly depending on tree species. The total fungal and saprotrophic OTU richness differences were mostly driven by $B.\ papyrifera$ plots, which had much lower soil fungal diversity than the other tree species studied. The fungal ectomycorrhizal OTU richness differences by tree species were explained by the non-ectomycorrhizal species ($A.\ negundo$, $A.\ rubrum$, and $J.\ virginiana$), which harbored a limited diversity of ectomycorrhizal fungi.

3.2. Effect of necromass type and tree species on necromass decomposition rates

Necromass decomposition rates (% of initial dry mass remaining) were significantly affected by necromass type (P < 0.001; Fig. 1a), with

the amount of low melanin necromass remaining being two times lower than for high melanin necromass. Tree species (P = 0.52) and the interaction between necromass type \times tree species (P = 0.99) did not significantly influence fungal necromass decomposition rates (see Fig. S3 for the amount of necromass mass remaining averaged by tree species). Linear mixed-effect models assessing the differences in necromass decomposition rates also did not reveal a significant effect on tree phylogeny (angiosperm vs. gymnosperm, P = 0.93), mycorrhization association (arbuscular mycorrhizal vs. ectomycorrhizal, P = 0.47), or the interaction between tree phylogeny and mycorrhizal association (P = 0.93), when controlling for tree species as a random factor (Table S2). There was, however, a significant positive correlation between low and high melanin necromass decomposition rates incubated across forest plots, such that if necromass with low melanin decomposed quickly in a given plot, necromass with high melanin did as well, and vice versa (R² = 0.39, P < 0.001, Fig. 1b).

3.3. Drivers of decomposition rates for low versus high melanin necromass

For both necromass types, none of the edaphic parameters (soil pH, moisture, and temperature) or plant traits (fine-root density, and fineroot and leaf tannin concentrations) significantly predicted decomposition rates (Fig. 2). However, total bacterial OTU richness and bacterial oligotrophic OTU richness were both found to be significant predictors of low melanin necromass decomposition rates. This result, based on multimodel inference, was confirmed using linear regressions showing significant negative correlations between the total soil bacterial (R^2 0.25, P = 0.002) and oligotrophic OTU richness ($R^2 = 0.22, P = 0.004$), with the amount of low melanin necromass remaining (Fig. 3a and b). Additionally, for both necromass types, the OTU composition of the soil fungal communities (PCo2) was the main predictor of fungal necromass decomposition. This pattern was also confirmed by significant Pearson's correlations between the fungal community structure and necromass mass remaining (low melanin: $R^2 = 0.22$, P = 0.004; high melanin: $R^2 =$ 0.24, P = 0.002, Fig. 3c).

Identifying that the structure of the soil fungal communities, but not the bacterial communities, predicted fungal necromass decay rates, canonical correlation analysis (CCA) was applied to further examine the relationships between the relative abundance of fungal genera and the decomposition rates of low and high melanin necromass. The CCA focused on the most abundant soil fungal genera and revealed that the low and high melanin necromass mass remaining vectors were not entirely parallel. Still, these vectors pointed in the same direction, suggesting that, at least partially, different microbial communities might be associated with necromass decomposition rates (Fig. 4). Fungal genera such as *Metarhizium*, *Scleroderma*, and *Thelephora* were all associated with greater mass loss for the low melanin necromass, while

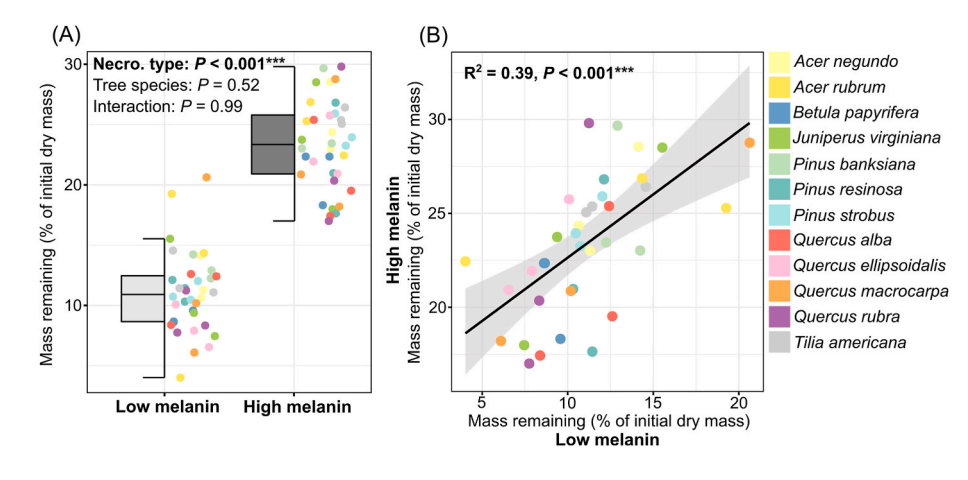


Fig. 1. (a) Fungal necromass mass remaining (% of initial dry mass) after incubation in forest soil depending on necromass type (low and high melanin) and tree species (A. negundo, A. rubrum, B. papyrifera, J. virginiana, P. banksiana, P. resinosa, P. strobus, Q. alba, Q. ellipsoidalis, Q. macrocarpa, Q. rubra, and T. Americana). The effect of necromass type and tree species and their interaction on necromass decomposition rate was assessed using a two-way analysis of variance (*, P < 0.05; **, P < 0.01; ***, P < 0.001). (b) Relationship between low and high melanin necromass mass remaining (% of initial dry mass) incubated at the same forest plot colored by the tree species (A. negundo, A. rubrum, B. papyrifera, J. virginiana, P. banksiana, P. resinosa, P. strobus, Q. alba, Q. ellipsoidalis, Q. macrocarpa, Q. rubra, and T. Americana) (Pearson's correlation; *, P < 0.05; **, P < 0.01; ***, P < 0.001). Shading represents the 95% confidence interval.

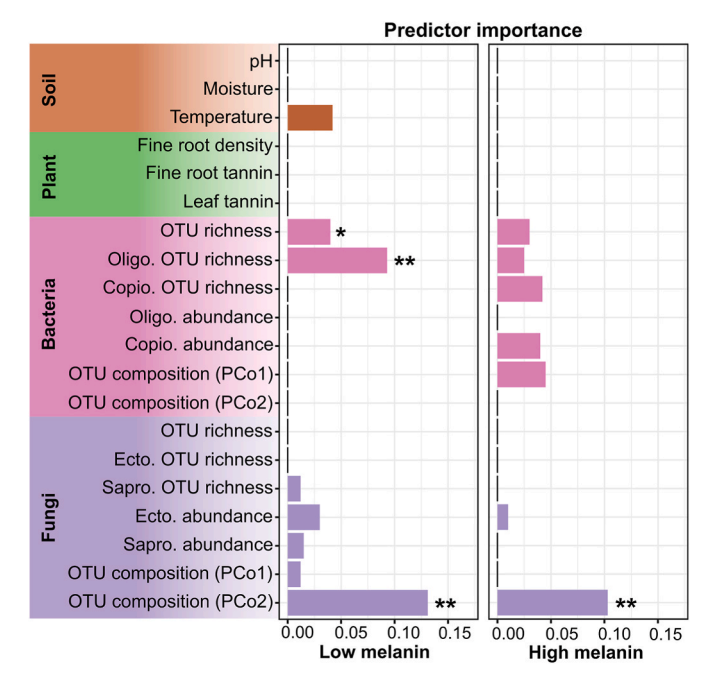


Fig. 2. Relative importance of predictors for the necromass decomposition rate (% of initial dry mass remaining) for low melanin (n=32) and high melanin (n=32) necromass types. Predictors were colored by categories (edaphic = brown, plant = green, bacteria = pink, and fungi = purple). Asterisks indicate a significant correlation based on the averaged model coefficients (*, P < 0.05; **, P < 0.01; ***, P < 0.001).

Pseudogymnascus and Wilcoxina were related to acceleration of high melanin necromass decomposition (Fig. 4). Exophiala was associated with substantial necromass mass losses for both low and high melanin necromass. Finally, Meliniomyces was associated with a deceleration in low melanin necromass decomposition.

3.4. Relationships between soil C and N concentrations and fungal necromass decay rates

There was no significant effect of tree species on soil C (P=0.054) or N (P=0.13) concentrations in the 0–20 cm soil layers (Fig. S4). However, there were significant positive correlations between the mass remaining of the low melanin fungal residues and soil C ($R^2=0.21$, P=0.005) as well as N concentrations ($R^2=0.16$, P=0.014) (Fig. 5). The

amount of high melanin necromass remaining post-incubation and soil C and N concentrations followed the same positive trends, but were only marginally significant (P < 0.10).

4. Discussion

Our study represents the first to systematically compare the extrinsic drivers of fungal necromass decomposition across a diverse range of forest types sharing similar pedoclimatic conditions. Specifically, using a common garden experiment with plots planted with different tree species to modulate edaphic parameters, tree traits, and soil microbial communities, we were able to evaluate the respective effects of a range of abiotic and biotic extrinsic factors on the decomposition of contrasting fungal necromass types. We confirm the strong impact of the initial chemical quality of the fungal residues on their decomposability, regardless of decomposition environment, but, surprisingly, found no significant influence of tree species on necromass decomposition rates. Instead, at the plot level, we identified the richness and the composition of the soil bacterial and fungal communities, rather than edaphic parameters and plant traits, as drivers of necromass decay. In combination with the intrinsic role of necromass chemistry, these results indicate that soil microbial communities represent the primary extrinsic driver of fungal necromass decomposition rates at local scales.

4.1. Necromass chemical properties, not tree species, drive necromass decay rates

As we postulated, the initial quality of the fungal necromass affected the decomposition rates, with the mass remaining of high melanin necromass twice as high as that of the low melanin necromass type. Our results paralleled studies comparing chemically distinct necromass types that consistently found greater retention of melanized necromass than non-melanized residues (Fernandez and Koide, 2014; Fernandez and Kennedy, 2018; Fernandez et al., 2019; See et al., 2021). The persistence of dead melanized mycelia might be associated with the intrinsic resistance of melanin to microbial degradation (Day and Bulter, 1998). Still, melanin may also reduce the accessibility for the microbial degradation of more labile compounds composing the fungal cell walls, such as the glucan, mannan, and chitin polymers (Bull 1970; Ryan et al., 2020). Importantly, we found a strong relationship between the decomposition rates of low and high melanin necromass types across plots, explaining around 40% of the variation in mass remaining. This indicates that while a substantial fraction of fungal necromass decay rates is linked to necromass quality, another fraction, likely composed of labile compounds (e.g., trehalose, glycogen, storage proteins etc.), is largely independent

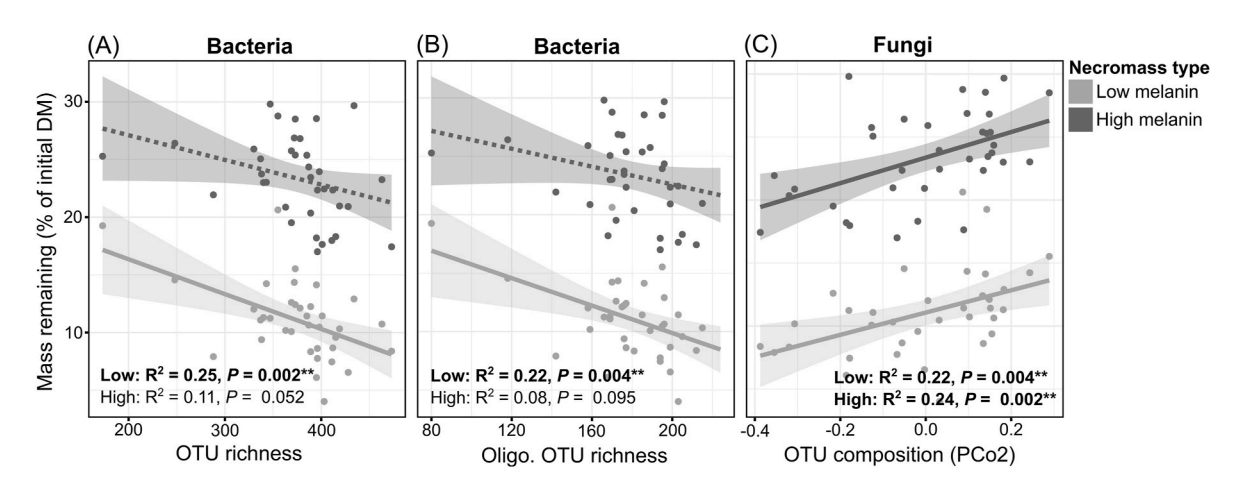


Fig. 3. Relationships between the necromass decomposition rate (% of initial dry mass remaining) and (a) bacterial OTU richness, (b) oligotrophic bacterial OTU richness, and (c) fungal OTU composition (PcO2) for the low and high melanin necromass types (Pearson's correlation; *, P < 0.05; **, P < 0.01; ***, P < 0.001). Dashed line indicates marginally significant correlation (P < 0.1). Shading represents the 95% confidence interval.

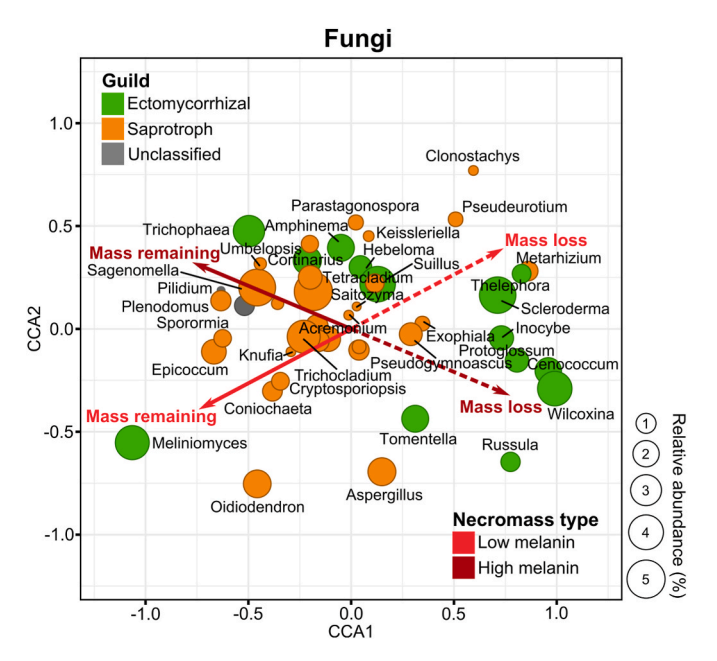


Fig. 4. Canonical correspondence analyses (CCA) with the 50 most abundant soil fungal genera. Fungal genera were colored depending on their associated functional group (ectomycorrhizal, saprotroph or unclassified). The size of the bubbles is proportional to the averaged relative abundance of each genus. Vectors illustrate the associations of fungal genera with the necromass decomposition rate (% of initial dry mass remaining) for low melanin and high melanin necromass types. Only mass remaining vectors were used for the canonical correspondence analyses, and symmetric mass loss vectors were plotted for interpretation purposes.

of necromass type.

Surprisingly, we did not detect any tree species effect associated with microclimatic soil modifications (i.e., soil moisture and temperature) and tree trait variations (i.e., root density and root tannins) on necromass decomposition rates, contradicting our first and second predictions. Multimodel inference confirmed those observations, with none of the edaphic parameters and tree traits significantly predicting necromass decomposition rates for either necromass type, despite large disparities in the amount of necromass remaining within necromass types. These negative results cannot be attributed to a lack of environmental gradients, given that both the soil moisture and temperature, as well as fine root density and tannin content, varied substantially at the plot level. Regarding the microclimatic soil parameters, it is possible

that the temperature and moisture ranges caused by the tree species were too narrow to induce significant changes in necromass decomposition rates. For example, in our study, the maximum average difference in temperature between two tree species (A. negundo vs. P. strobus plots) was 2.3 °C, while in a warming experiment, Fernandez et al. (2019) only started observing differences in fungal necromass decomposition at +4.5 °C compared with the control treatment. Our results suggest that microclimatic parameters induced by different tree species on necromass decomposition rates are likely minor. This supposition also aligns with the earlier observational findings of Beidler et al. (2020), which showed a lack of a vegetation-type effect on fungal necromass decomposition. Because we only assessed microclimatic parameters at one time point over the course of the experiment, however, continuous soil temperature and moisture measurements using dedicated data loggers will be necessary to fully capture the potential effects of forest microclimatic effects on necromass decay rates.

Concerning plant traits, we speculate that our incubation time of five months might have been too short, even though it reached the late stages of necromass decomposition, to observe the effect of root-derived tannin on fungal residue decay dynamics. In particular, working in a boreal forest, Adamczyk et al. (2019) only started observing the consequences of the accumulation of tannins in necromass after 18 months of incubation. Thus, we speculate that the adsorption of tannins on necromass might be a relatively slow process in forest soils. It is also possible that some microbial degradation processes that only happen in the late stages of necromass decomposition make fungal residues more reactive toward binding plant-derived tannins.

4.2. Soil bacterial richness predicts fungal necromass decomposition rates

In partial disagreement with our third hypothesis, neither soil fungal functional group abundance nor diversity was identified as affecting necromass decay rates. Alternatively, bacterial richness significantly predicted necromass decay rates, with both total bacterial and oligotrophic richnesses negatively correlating with the amount of low melanin necromass remaining. This necromass type-specific result suggests the roles of bacteria in the degradation of highly melanized and recalcitrant necromass might be limited in soils. In support of this possibility, Starke et al. (2020) discovered that three of four bacterial genera colonizing necromass had weak growth on the cell-wall fraction compared with whole fungal residues. Our results also notably align with research determining that low soil bacterial diversity impeded the decomposition of wheat (Maron et al., 2018) and maize (Chiba et al., 2021) litters using laboratory microbial extinction-dilution approaches. This suggests that the positive links between soil bacterial diversity and organic matter decomposition rates proposed for plant residues may be

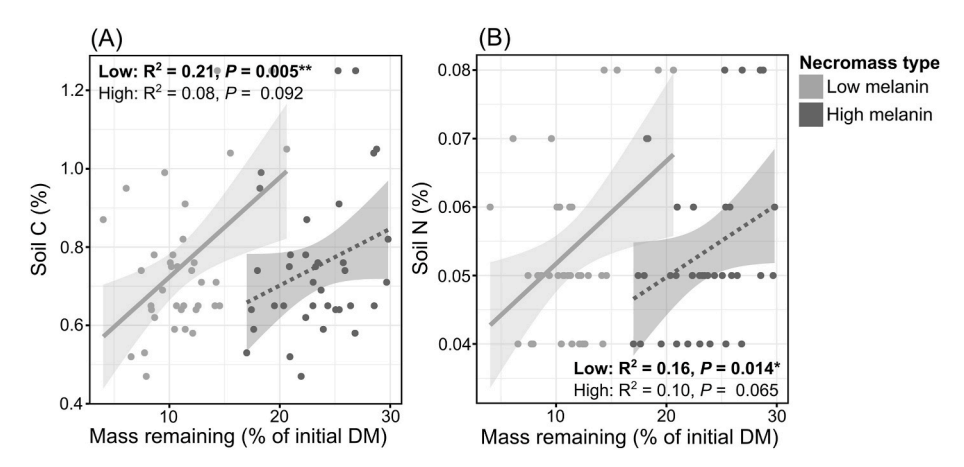


Fig. 5. Relationships between soil (a) C and (b) N concentrations (% in the 0–20 cm layer) and the necromass decomposition rate (% of initial dry mass remaining incubating in the 0–5 cm layer) for the low and high melanin necromass types (Pearson's correlation; *, P < 0.05; **, P < 0.01; ***, P < 0.001). Dashed line indicates a marginally significant correlation (P < 0.1). Shading represents the 95% confidence interval.

extended to microbial necromass.

4.3. Soil fungal microbial community composition drives fungal necromass decomposition rates

Among all the extrinsic factors considered, the composition of the soil fungal communities most significantly predicted the decomposition rates of both low and high melanin necromass types. Most of the fungal genera we found to be associated with significant necromass mass losses were previously categorized as colonizers of fungal residues, such as Pseudogymnoascus, Metarhizium, Exophiala, Thelephora, Wilcoxina, and Scleroderma (Beidler et al., 2020; Brabcová et al., 2018; López-Mondéjar et al., 2018; Maillard et al., 2020, 2023). These findings show that soils natively enriched in fungal necromass decomposers might facilitate the faster turnover of these residues, likely due to an increased functional potential for fungal compound degradation. This is notably reinforced by the fact that Pseudogymnoascus and Metarhizium have been extensively characterized as efficient degraders of chitin, one of the main components of fungal necromass (Junges et al., 2014; Martinović et al., 2022; St Leger et al., 1991). Regarding the genus Exophiala, although there is currently no direct evidence to support its ability to decompose fungal necromass, existing studies that illustrate its effectiveness in breaking down diverse polymers might imply that it could also efficiently degrade molecules associated with necromass (Ide-Pérez et al., 2020; Middelhoven 1993). However, it is more challenging to explain how ectomycorrhizal fungi, such as Thelephora, Wilcoxina, and Scleroderma, were responsible for accelerated necromass decomposition under our experimental conditions, as none have been previously defined as efficient organic matter degraders (Lindahl et al., 2021; Miyauchi et al., 2020). Given that root exudates are transferred to soil bacteria through ectomycorrhizal hyphae (Gorka et al., 2019), we speculate that these ectomycorrhizal fungal genera may prime necromass decomposition by efficiently transferring labile carbon sources to necromass-degrading bacteria.

4.4. Fungal necromass decay rates are coupled with soil C and N pools

In disagreement with our fourth prediction, and despite studies showing that more soil C is stored in ectomycorrhizal forests compared with their arbuscular mycorrhizal counterparts (Soudzilovskaia et al., 2019; Steidinger et al., 2019), we did not identify a tree species effect on the soil C concentration in our experimental settings. As soil C concentrations were measured six years after the plantation of the trees, it is possible that this relatively short time lap was insufficient to observe a strong tree species' effect. However, in agreement with the second part of our fourth prediction, we found a positive relationship between the soil C and N concentrations and the amount of fungal residue remaining after the decomposition period of five months for both necromass types. In other words, plots where fungal necromass tended to accumulate in its particulate form (i.e., high necromass mass remaining within the mycobags) harbored high soil C and N concentrations. This suggests a strong coupling between the fungal necromass decomposition rates and the soil C and N stocks, paralleling research showing a critical role of the microbial residues in the soil C and N cycles (Liang et al., 2019; Liu et al., 2021; Wang et al., 2021).

4.5. Limitations

The lack of any significant tree species effects on necromass decomposition rates might reflect the nature of our necromass incubations. Specifically, many previous studies have found that as the distance between tree roots and the soil increases, the plant-structuring effects on the soil microbial communities also decrease (Coleman-Derr et al., 2016; Mendes et al., 2014). As we conducted our incubations in bulk soil, with mesh bags putatively separating the substrates from any potential roots and associated rhizospheres, our experimental conditions

might have minimized the role of tree traits and associated fungi in necromass decomposition. Since fungal biomass is higher in the rhizosphere than in bulk soil (Guo et al., 2015), a large part of the fungal residue turnover might occur near the roots (See et al., 2022). Consequently, the drivers of fungal necromass decomposition in bulk and rhizospheric soils might differ. Additionally, we must note that the fungal primer pair we used did not efficiently recover arbuscular mycorrhizal fungi, so we might have neglected their role in mediating mycelial residue degradation processes. Finally, while we decided to use the attributes of soil communities at the beginning of the experiment as potential predictors of fungal necromass decomposition, it is likely that part of these communities, and notably mycorrhizal fungi, might have experienced changes in biomass production during the incubation time (Castaño et al., 2017; Shigyo et al., 2019). Therefore, future studies should develop methods to monitor the decay rates of fungal residues in close contact with plant roots in situ. They should also use a combination of generalist and arbuscular mycorrhizal fungi-specific primer pairs to fully capture soil fungal diversity for arbuscular mycorrhizal trees, and sample soil communities at different times during necromass degradation to account for seasonal microbial community changes.

5. Conclusions

The current study has confirmed the intrinsic role of the initial chemical composition of fungal necromass in its decay trajectories across a wide range of North American tree species, with highly melanized residues decomposing more slowly than lowly melanized residues. While we found no effect of soil microclimatic parameters or tree traits on the decomposition of fungal necromass, we have demonstrated that the main extrinsic factors predicting necromass accumulation are attributes of soil microbial communities. Most notably, bacterial richness was associated with low melanin necromass decomposition, while the composition of the fungal communities predicted both low and high melanin necromass decay rates. As a result, we propose that bacterial functional redundancy may be an important driver of fungal necromass decomposition. In addition, soil communities enriched in fungal necromass decomposers, by being functionally preadapted for the degradation of this substrate, might accelerate the decomposition of necromass. Finally, based on our results showing that fungal necromass degradation and soil C and N concentrations are coupled, we emphasize that identifying the microbial factors driving necromass decomposition in conjunction with necromass chemical properties will help in better incorporating microbial-derived organic matter components into soil biogeochemical models.

Author's contributions

F.M. coordinated the project. F.M. and P.G.K. designed the study. The experiments were conducted by F.M., B.B., C.R.S, M.P., S.A., and B. A. All the authors analyzed and interpreted the data. F.M. wrote the manuscript with help from P.G.K.

Declaration of competing interest

We state that there is no conflict of interest.

Data availability

Data will be made available on request.

Acknowledgements

We thank the editor, Marie Sauvadet, and the four anonymous reviewers for their valuable comments and suggestions, which contributed to improving the quality of the manuscript. The authors thank B. Tanner for assistance with 16S and ITS library preparation. The FAB experiment

was established and maintained with support from the Cedar Creek Long Term Ecological Research program (DEB-1234162, DEB-1831944). We also acknowledge the Joint Genome Initiative "Defining the Populus Microbiome" Project, from which the *M. bicolor* isolate used for necromass was derived.

Appendix A. Supplementary data

Supplementary data to this article can be found online at $\frac{https:}{doi.}$ org/10.1016/j.soilbio.2023.109124.

References

- Adamczyk, B., Kitunen, V., Smolander, A., 2008. Protein precipitation by tannins in soil organic horizon and vegetation in relation to tree species. Biology and Fertility of Soils 45, 55–64.
- Adamczyk, B., Simon, J., Kitunen, V., Adamczyk, S., Smolander, A., 2017. Tannins and their complex interaction with different organic nitrogen compounds and enzymes: old paradigms versus recent advances. Chemistry Open 6, 610–614.
- Adamczyk, B., Sietiö, O.M., Biasi, C., Heinonsalo, J., 2019. Interaction between tannins and fungal necromass stabilizes fungal residues in boreal forest soils. New Phytologist 223, 16–21.
- Angst, G., Mueller, K.E., Nierop, K.G.J., Simpson, M.J., 2021. Plant- or microbial-derived? A review on the molecular composition of stabilized soil organic matter. Soil Biology and Biochemistry 156, 108189.
- Bates, D., Maechler, M., Bolker, B., Walker, S., 2015. Fitting linear mixed-effects models using lme4. Journal of Statistical Software 67, 1–48.
- Beidler, K.V., Phillips, R.P., Andrews, E., Maillard, F., Mushinski, R.M., Kennedy, P.G., 2020. Substrate quality drives fungal necromass decay and decomposer community structure under contrasting vegetation types. Journal of Ecology 108, 1845–1859.
- Beidler, K.V., Oh, Y.E., Pritchard, S.G., et al., 2021. Mycorrhizal roots slow the decay of belowground litters in a temperate hardwood forest. Oecologia 197, 743–755.
- Brabcová, V., Novakova, M., Davidova, A., Baldrian, P., 2016. Dead fungal mycelium in forest soil represents a decomposition hotspot and a habitat for a specific microbial community. New Phytologist 210, 1369–1381.
- Brabcová, V., Štursova, M., Baldrian, P., 2018. Nutrient content affects the turnover of fungal biomass in forest topsoil and the composition of associated microbial communities. Soil Biology and Biochemistry 118, 187–198.
- Bradford, M.A., Berg, B., Maynard, D.S., Wieder, W.R., Wood, S.A., 2016. Understanding the dominant controls on litter decomposition. Journal of Ecology 104, 229–238.
- Buckeridge, K.M., La Rosa, A.F., Mason, K.E., Whitaker, J., McNamara, N.P., Grant, H.K., et al., 2020. Sticky dead microbes: rapid abiotic retention of microbial necromass. Soil Biology and Biochemistry 149, 107929–107933.
- Buckeridge, K., Creamer, C., Whitaker, J., 2022. Deconstructing the microbial necromass continuum to inform soil carbon sequestration. Functional Ecology 36, 1396–1410.
- Bull, A.T., 1970. Inhibition of polysaccharases in relation by Melanin: to mycolysis enzyme inhibition. Archives of Biochemistry and Biophysics 345e356.
- Burnham, K.P., Anderson, D.R., 2002. Model Selection and Multimodel Inference: a Practical Information-Theoretic Approach, second ed. Springer-Verlag, New York.
- Callahan, B.J., McMurdie, P.J., Rosen, M.J., Han, A.W., Johnson, A.J.A., Holmes, S.P., 2016. DADA2. High-resolution sample inference from Illumina amplicon data. Nature Methods 13, 581–583.
- Caporaso, J.G., Lauber, C.L., Walters, W.A., Berg-Lyons, D., Huntley, J., Fierer, N., Owens, S.M., Betley, J., Fraser, L., Bauer, M., Gormley, N., Gilbert, J.A., Smith, G., Knight, R., 2012. Ultra-high-throughput microbial community analysis on the Illumina HiSeq and MiSeq platforms. ISME Journal 6, 1621–1624.
- Castaño, C., Alday, J.G., Parladé, J., Pera, J., Martínez de Aragón, J., Bonet, J.A., 2017. Seasonal dynamics of the ectomycorrhizal fungus Lactarius vinosus are altered by changes in soil moisture and temperature. Soil Biology and Biochemistry 115, 253–260.
- Chiba, A., Uchida, Y., Kublik, S., Vestergaard, G., Buegger, F., Schloter, M., Schulz, S., 2021. Soil bacterial diversity is positively correlated with decomposition rates during early phases of maize litter decomposition. Microorganisms 9, 357.
- Clemmensen, K.E., Finlay, R.D., Dahlberg, A., Stenlid, J., Wardle, D.A., Lindahl, B.D., 2015. Carbon sequestration is related to mycorrhizal fungal community shifts during long-term succession in boreal forests. New Phytologist 205, 1525–1536.
- Coleman-Derr, D., Desgarennes, D., Fonseca-Garcia, C., Gross, S., Clingenpeel, S., Woyke, T., et al., 2016. Plant compartment and biogeography affect microbiome composition in cultivated and native Agave species. New Phytologist 209, 798–811.
- Cotrufo, M.F., Wallenstein, M.D., Boot, C.M., Denef, K., Paul, E., 2013. The microbial efficiency-matrix stabilization (MEMS) framework integrates plant litter decomposition with soil organic matter stabilization: do labile plant inputs form stable soil organic matter? Global Change Biology 19, 988–995.
- Fanin, N., Bezaud, S., Sarneel, J.M., et al., 2020. Relative importance of climate, soil and plant functional traits during the early decomposition stage of standardized litter. Ecosystems 23, 1004–1018.
- Fernandez, C.W., Kennedy, P.G., 2016. Revisiting the 'Gadgil effect': do interguild fungal interactions control carbon cycling in forest soils? New Phytologist 209, 1382–1394.
- Fernandez, C.W., Kennedy, P.G., 2018. Melanization of mycorrhizal fungal necromass structures microbial decomposer communities. Journal of Ecology 106, 468–479.

- Fernandez, C.W., Koide, R.T., 2014. Initial melanin and nitrogen concentrations control the decomposition of ectomycorrhizal fungal litter. Soil Biology and Biochemistry 77, 150–157.
- Fernandez, C.W., Heckman, K., Kolka, R., Kennedy, P.G., 2019. Melanin mitigates the accelerated decay of mycorrhizal necromass with peatland warming. Ecology Letters 22, 498–505.
- Gorka, S., Dietrich, M., Mayerhofer, W., Gabriel, R., Wiesenbauer, J., Martin, V., et al., 2019. Rapid transfer of plant photosynthates to soil bacteria via ectomycorrhizal hyphae and its interaction with nitrogen availability. Frontiers in Microbiology 10, 168.
- Grelet, G.A., Meharg, A.A., Duff, E.I., Anderson, I.C., Alexander, I.J., 2009. Small genetic differences between ericoid mycorrhizal fungi affect nitrogen uptake by *Vaccinium*. New Phytologist 18, 708–718.
- Grossman, J.J., Cavender-Bares, J., Hobbie, S.E., Reich, P.B., Montgomery, R.A., 2017. Species richness and traits predict overyielding in stem growth in an early-successional tree diversity experiment. Ecology 98, 2601–2614.
- Grossman, J.J., Cavender-Bares, J., Hobbie, S.E., 2020. Functional diversity of leaf litter mixtures slows decomposition of labile but not recalcitrant carbon over two years. Ecological Monographs 90, e01407.
- Guo, H.C., Wand, W.B., Luo, X.H., Wu, X.P., 2015. Characteristics of rhizosphere and bulk soil microbial communities in rubber plantations in Hainan island, China. Journal of Tropical Forest Science 27, 202–212.
- Hättenschwiler, S., Sun, T., Coq, S., 2019. The chitin connection of polyphenols and its ecosystem consequences. New Phytologist 223, 5–7.
- Ide-Pérez, M.R., Fernández-López, M.G., Sánchez-Reyes, A., Leija, A., Batista-García, R. A., Folch-Mallol, J.L., Sánchez-Carbente, R., 2020. Aromatic hydrocarbon removal by novel extremotolerant Exophiala and Rhodotorula spp. from an oil polluted site in Mexico. Journal of Fungi 6.
- Junges, Â., Boldo, J.T., Souza, B.K., Guedes, R.L.M., Sbaraini, N., Kmetzsch, L., et al., 2014. Genomic analyses and transcriptional profiles of the glycoside hydrolase family 18 genes of the entomopathogenic fungus *Metarhizium anisopliae*. PLoS One 9, e107864.
- Kästner, M., Miltner, A., Thiele-Bruhn, S., Liang, C., 2021. Microbial necromass in soils—linking microbes to soil processes and carbon turnover. Frontiers in Environmental Science 9, 756378.
- Kennedy, P.G., Maillard, F., 2022. Knowns and unknowns of the soil fungal necrobiome. Trends in Microbiology 31, 173–180.
- Li, H., Yang, S., Semenov, M.V., Yao, F., Ye, J., Bu, R., Ma, R., Lin, J., Kurganova, I., Wang, X., Deng, Y., Kravchenko, I., Jiang, Y., Kuzyakov, Y., 2021. Temperature sensitivity of SOM decomposition is linked with a K-selected microbial community. Global Change Biology 27, 2763–2779.
- Liang, C., Schimel, J.P., Jastrow, J.D., 2017. The importance of anabolism in microbial control over soil carbon storage. Nature Microbiology 2, 17105.
- Liang, C., Amelung, W., Lehmann, J., Kästner, M., 2019. Quantitative assessment of microbial necromass contribution to soil organic matter. Global Change Biology 25, 3578–3590.
- Lindahl, B.D., Kyaschenko, J., Varenius, K., Clemmensen, K.E., Dahlberg, A., Karltun, E., Stendahl, J., 2021. A group of ectomycorrhizal fungi restricts organic matter accumulation in boreal forest. Ecology Letters 24, 1341–1351.
- Liu, Y., Wang, G., Yu, K., Li, P., Xiao, L., Liu, G., 2018. A new method to optimize root order classification based on the diameter interval of fine root. Scientific Reports 8.
- Liu, Z., Liu, X., Wu, X., Bian, R., Liu, X., Zheng, J., Zhang, X., Cheng, K., Li, L., Pan, G., 2021. Long-term elevated CO2 and warming enhance microbial necromass carbon accumulation in a paddy soil. Biology and Fertility of Soils 57, 673–684.
- López-Mondéjar, R., Brabcova, V., Stursova, M., et al., 2018. Decomposer food web in a deciduous forest shows high share of generalist microorganisms and importance of microbial biomass recycling. ISME Journal 12, 1768–1778.
- Maillard, F., Schilling, J., Andrews, E., Schreiner, K.M., Kennedy, P., 2020. Functional convergence in the decomposition of fungal necromass in soil and wood. FEMS Microbiology Ecology 96, fiz209.
- Maillard, F., Kennedy, P.G., Adamczyk, B., et al., 2021. Root presence modifies the long-term decomposition dynamics of fungal necromass and the associated microbial communities in a boreal forest. Molecular Ecology 30, 1921–1935.
- Maillard, F., Jusino, M.A., Andrews, E., Moran, M., Vaziri, G.J., Banik, M.T., Fanin, N., Trettin, C.C., Lindner, D.L., Schilling, J.S., 2022a. Wood-decay type and fungal guild dominance across a North American log transplant experiment. Fungal Ecology 59, 101151.
- Maillard, F., Fernandez, C.W., Mundra, S., Heckman, K.A., Kolka, R.K., Kauserud, H., Kennedy, P.G., 2022b. Warming drives a 'hummockification' of microbial communities associated with decomposing mycorrhizal fungal necromass in peatlands. New Phytologist 234, 2032–2043.
- Maillard, F., Michaud, T.J., See, C.R., DeLancey, L.C., Blazewicz, S.J., Kimbrel, J.A., Pett-Ridge, J., Kennedy, P.G., 2023. Melanization slows the rapid movement of fungal necromass carbon and nitrogen into both bacterial and fungal decomposer communities and soils. mSystems, e00390-23.
- Maron, P.A., Sarr, A., Kaisermann, A., Lévêque, J., Mathieu, O., Guigue, J., Karimi, B., Bernard, L., Dequiedt, S., Terrat, S., et al., 2018. High microbial diversity promotes soil ecosystem functioning. Applied and Environmental Microbiology 84, 1–13.
- Martinović, T., Odriozola, I., Masínová, T., Bahnmann, B.D., Kohout, P., Sedlák, P., Merunková, K., Větrovský, T., Tomšovský, M., Ovaskainen, O., Baldrian, P., 2021. Temporal turnover of the soil microbiome composition is guild-specific. Ecology Letters 24, 2726–2738.
- Martinović, T., Mašínová, T., López-Mondéjar, R., Jansa, J., Štursová, M., Starke, R., Baldrian, P., 2022. Microbial utilization of simple and complex carbon compounds in a temperate forest soil. Soil Biology and Biochemistry 173, 108786.

- Mendes, L., Kuramae, E., Navarrete, A., et al., 2014. Taxonomical and functional microbial community selection in soybean rhizosphere. ISME Journal 8, 1577–1587.
- Middelhoven, W.J., 1993. Catabolism of benzene compounds by ascomycetous and basidiomycetous yeasts and yeastlike fungi. Antonie van Leeuwenhoek 63, 12–144.
- Miyauchi, S., Kiss, E., Kuo, A., et al., 2020. Large-scale genome sequencing of mycorrhizal fungi provides insights into the early evolution of symbiotic traits. Nature Communications 11. 5125.
- Nguyen, N.H., Song, Z., Bates, S.T., Branco, S., Tedersoo, L., Menke, J., Schilling, J.S., Kennedy, P.G., 2016. FUNGuild: an open annotation tool for parsing fungal community datasets by ecological guild. Fungal Ecology 20, 241–248.
- Oksanen, J., Blanchet, F.G., Kindt, R., Legendre, P., Minchin, P.R., O'Hara, R.B., et al., 2013. Vegan: Community Ecology Package, Version 2.0–7. R Package. Available: http://CRAN.R-project.org/package=vegan.
- Palmer, J.M., Jusino, M.A., Banik, M.T., Lindner, D.L., 2018. Non-biological synthetic spike-in controls and the AMPtk software pipeline improve mycobiome data. PeerJ 6, e4925
- Prescott, C.E., 2010. Litter decomposition: what controls it and how can we alter it to sequester more carbon in forest soils? Biogeochemistry 101, 133–149.
- R Core Team, 2020. R: A Language and Environment for Statistical Computing. R Foundation for Statistical Computing, Vienna, Austria. URL. http://www.R-project.org/.
- Ryan, M.E., Schreiner, K.M., Swenson, J.T., Gagne, J., Kennedy, P.G., 2020. Rapid changes in the chemical composition of degrading ectomycorrhizal fungal necromass. Fungal Ecology 45, 100922.
- Santalahti, M., Sun, H., Jumpponen, A., Pennanen, T., Heinonsalo, J., 2016. Vertical and seasonal dynamics of fungal communities in boreal Scots pine forest soil. FEMS Microbiology Ecology 92, fiw170.
- Schweigert, M., Herrmann, S., Miltner, A., Fester, T., Kästner, M., 2015. Fate of ectomycorrhizal fungal biomass in a soil bioreactor system and its contribution to soil organic matter formation. Soil Biology and Biochemistry 88, 120–127.
- See, C.R., Fernandez, C.W., Conley, A.M., DeLancey, L.C., Heckman, K.A., Kennedy, P.G., Hobbie, S.E., 2021. Distinct carbon fractions drive a generalizable twopool model of fungal necromass decomposition. Functional Ecology 35, 796–806.
- See, C.R., Keller, A.B., Hobbie, S.E., Kennedy, P.G., Weber, P.K., Pett-Ridge, J., 2022. Hyphae move matter and microbes to mineral microsites: integrating the hyphosphere into conceptual models of soil organic matter stabilization. Global Change Biology 28, 2527–2540.
- Shigyo, N., Umeki, K., Hirao, T., 2019. Seasonal dynamics of soil fungal and bacterial communities in cool-temperate montane forests. Frontiers in Microbiology 10.
- Siletti, C.E., Zeiner, C.A., Bhatnagar, J.M., 2017. Distributions of fungal melanin across species and soils. Soil Biology and Biochemistry 113, 285–293.

- Sokol, N.W., Slessarev, E., Marschmann, G.L., Nicolas, A., Blazewicz, S.J., Brodie, E.L., Firestone, M.K., Foley, M.M., Hestrin, R., Hungate, B.A., Koch, B.J., Stone, B.W., Sullivan, M.B., Zablocki, O., , LLNL Soil Microbiome Consortium, Pett-Ridge, J., 2022. Life and death in the soil microbiome: how ecological processes influence biogeochemistry. Nature Reviews Microbiology 20, 415–430.
- Soudzilovskaia, N.A., van Bodegom, P.M., Terrer, C., van't Zelfde, M., McCallum, I., McCormack, L.M., Fisher, J.B., Brundrett, M.C., de Sá, N.C., Tedersoo, L., 2019. Global mycorrhizal plant distribution linked to terrestrial carbon stocks. Nature Communications 10. 1–10.
- St Leger, R.J., Cooper, R.M., Charnley, A.K., 1991. Characterization of chitinase and chitobiase produced by the entomopathogenic fungus *Metarhizium anisopliae*. Journal of Invertebrate Pathology 58, 415–426.
- Starke, R., Morais, D., Vetrovsky, T., Lopez Mondejar, R., Baldrian, P., Brabcova, V., 2020. Feeding on fungi: genomic and proteomic analysis of the enzymatic machinery of bacteria decomposing fungal biomass. Environmental Microbiology 22, 4604–4619
- Steidinger, B.S., Crowther, T.W., Liang, J., Van Nuland, M.E., Werner, G.D.A., Reich, P. B., Nabuurs, G.J., de-Miguel, S., Zhou, M., Picard, N., et al., 2019. Climatic controls of decomposition drive the global biogeography of forest-tree symbioses. Nature 569, 404–408.
- Taylor, D.L., Walters, W.A., Lennon, N.J., Bochicchio, J., Krohn, A., Caporaso, J.G., Pennanen, T., 2016. Accurate estimation of fungal diversity and abundance through improved lineage-specific primers optimized for Illumina amplicon sequencing. Applied and Environmental Microbiology 82, 7217–7226.
- Throckmorton, H.M., Bird, J.A., Dane, L., Firestone, M.K., Horwath, W.R., 2012. The source of microbial C has little impact on soil organic matter stabilisation in forest ecosystems. Ecology Letters 15, 1257–1265.
- van der Wal, A., Bloem, J., Mulder, C., de Boer, W., 2009. Relative abundance and activity of melanized hyphae in different soil ecosystems. Soil Biology and Biochemistry 41, 417–419.
- Vivanco, L., Austin, A.T., 2008. Tree species identity alters forest litter decomposition through long-term plant and soil interactions in Patagonia, Argentina. Journal of Ecology 96, 727–736.
- Wang, B., An, S., Liang, C., Liu, Y., Kuzyakov, Y., 2021. Microbial necromass as the source of soil organic carbon in global ecosystems. Soil Biology and Biochemistry 162, 108422.
- Wieder, W.R., Allison, S.D., Davidson, E.A., Georgiou, K., Hararuk, O., He, Y., Hopkins, F., Luo, Y., Smith, M.J., Sulman, B., Todd-Brown, K., Wang, Y.P., Xia, J., Xu, X., 2015. Explicitly representing soil microbial processes in Earth system models. Global Biogeochemical Cycles 29, 1782–1800.